RMetS

Royal Meteorological Society

Does the recent warming hiatus exist over Northern Asia for winter wind chill temperature?

Ying Ma,[a,b] Rui Mao,[a]* Sheng-Hui Feng,[c] Dao-Yi Gong[a] and Seong-Joong Kim[d]

[a] *State Key Laboratory of Earth Surface Processes and Resource Ecology, Beijing Normal University, China*
[b] *Academy of Disaster Reduction and Emergency Management Ministry of Civil Affairs & Ministry of Education, Beijing Normal University, China*
[c] *Geography Department, Tangshan No.1 High School, China*
[d] *Division of Polar Climate Change, Korea Polar Research Institute, Incheon, South Korea*

ABSTRACT: Wind chill temperature (WCT) describes the joint effect of wind velocity and air temperature on exposed body skin and could support policymakers in designing plans to reduce the risks of notably cold and windy weather. This study examined winter WCT over Northern Asia during 1973–2013 by analysing *in situ* station data. The winter WCT warming rate over the Tibetan Plateau (TP) slowed during 1999–2013 ($-0.04\,°\text{C}\,\text{decade}^{-1}$) compared with that of during 1973–1998 ($0.67\,°\text{C}\,\text{decade}^{-1}$). The winter WCT warming hiatus has also been observed in the remainder of Northern Asia with trends of $1.11\,°\text{C}\,\text{decade}^{-1}$ during 1973–1998 but $-1.02\,°\text{C}\,\text{decade}^{-1}$ during 1999–2013, except for the Far East (FE) of Russia, where the winter WCT has continued to heat up during both the earlier period of 1973–1998 ($0.54\,°\text{C}\,\text{decade}^{-1}$) and the recent period of 1999–2013 ($0.75\,°\text{C}\,\text{decade}^{-1}$). The results indicate that the influence of temperature on winter WCT is greater than that of wind speed over Northern Asia. Atmospheric circulation changes associated with air temperature and wind speed were analysed to identify the causes for the warming hiatus of winter WCT over Northern Asia. The distributions of sea-level pressure and 500-hPa height anomalies during 1999–2013 transported cold air from the high latitudes to middle latitudes, resulting in low air temperature over Northern Asia except for the FE of Russia. Over the TP, the increase in wind speed offset the increase in air temperature during 1999–2013. For the FE, the southerly wind from the Western Pacific drove the temperature up during the 1999–2013 period through warm advection.

KEY WORDS   wind chill temperature; Northern Asia; warming hiatus

Received 7 April 2016; Revised 29 August 2016; Accepted 31 August 2016

1. Introduction

Low air temperature and gale weather in winter poses a hazard because it can harm exposed human skin (Danielsson, 1996). The wind chill temperature (WCT) index or wind chill index is a measurement used to evaluate the joint effect of high wind velocity and low temperature on exposed body skin. A low (high) WCT indicates cold and windy (warm and less windy) weather. Asia is the most populated continent in the world and many people in this region experience cold and windy weather in the winter season, particularly in northeast Asia and Siberia (e.g. Analitis *et al.*, 2008; Baccini *et al.*, 2008; Rehill *et al.*, 2015). For example, it was reported that many countries in Asia experienced record low temperatures in January 2016, with over 100 known deaths due to hypothermia and cardiac arrest and more than 10 000 travellers stranded at the airport in South Korea (Tiffany, 2016). Therefore, it is important to examine the changes in WCT over Asia to gather information on potential hazards to human life and

to support policymakers in designing policies for adaptation to the changing climate.

Many studies have analysed the changes in WCT over regions of the world. Certain authors examined the diurnal, monthly and annual variation of WCT and suggested reasons for those changes in WCT. For example, Balafoutis (1989) described the diurnal WCT over Thessaloniki, Greece using Siple-Passel's formula (Siple and Passel, 1945) and indicated that surface air temperature plays a dominant role in WCT. Czarnecka and Michalska (2007) studied the diurnal values of the wind chill index over the Szczecin Lowlands and believed that atmospheric thaw predominantly controls the changes in WCT. Other studies analysed the long-term WCT and suggested that global warming might be the reason for the increasing trend in WCT from the regional scale to the continental scale. For example, certain high-latitude regions in North America (Keimig and Bradley, 2002), Northern Asia (Sheng-hui Feng, private communication) and China (Feng *et al.*, 2009) have experienced an increasing trend in WCT during recent decades according to the increase in surface temperature in association with global warming.

Recently, the Intergovernmental Panel on Climate Change Fifth Assessment Report noted that global warming has slowed during the winter season over the most

* Correspondence to: R. Mao, State Key Laboratory of Earth Surface Processes and Resource Ecology, Beijing Normal University, Beijing 100875, China. E-mail: mr@bnu.edu.cn

recent 15 years (1998–2012) (Easterling and Wehner, 2009; Fyfe *et al.*, 2013; Kosaka and Xie, 2013; Trenberth *et al.*, 2014; Fyfe *et al.*, 2016). For example, the winter mean maximum (minimum) temperature shows an increasing trend of 0.335 °C decade^{-1} (0.615 °C decade^{-1}) over China for the period 1961–1997, but this trend falls to −0.348 °C decade^{-1} (−0.805 °C decade^{-1}) from 1998 to 2012 (Li *et al.*, 2015). In addition, variations in wind velocity over China also show different patterns before and after 1998, i.e. a long-term decreasing trend before 1998 and a nearly zero trend after (Lin *et al.*, 2013). The combined effect of the increasing (decreasing) trend in air temperature together with the decreasing (nearly zero) trend in wind velocity before (after) 1998 over China indicates that an increasing (decreasing) WCT trend might have occurred over China before (after) 1998. This observation indicates that a warming slowdown (i.e. hiatus) of WCT exists in recent decades after 1998 compared with the period before 1998 when a warming trend of WCT occurred. Considering the widespread slowdown in the warming rate of surface air temperature and the nearly invariant wind speed in the world over the recent decade (Intergovernmental Panel on Climate Change [IPCC], 2013; Vautard *et al.*, 2010), we hypothesized that a warming hiatus of WCT also existed over Northern Asia over the recent decade in addition to China. In this study, we analyse the changes in the WCT index over Northern Asia since 1973 to examine whether a warming hiatus of the winter WCT occurred from 1998 to 2013. Section 2 describes the data and methods applied. The trend in winter WCT over Northern Asia and the contribution of air temperature and wind speed to the changes in winter WCT are discussed in Section 3. In Section 4, circulation changes in association with WCT changes are analysed to interpret the WCT variations over Northern Asia. Finally, a summary is presented in Section 5.

2. Data and methods

A daily meteorological data set containing air temperature and wind speed records was analysed in this study. This data set is available for the period 1973–2013 from NOAA's National Climate Data Center (NCDC) Global Surface Summary of the Day data set (ftp://ftp.ncdc.noaa.gov/pub/data/gsod/). The daily data are transformed to monthly data by averaging the daily values. In addition, we analysed the monthly reanalysis data offered by the National Centers for Environmental Prediction-National Center for Atmospheric Research (NECP/NCAR) with a horizontal resolution of 2.5° × 2.5° (Kalnay *et al.*, 1996) to investigate the circulation changes that influence WCT variations. This data set extends from 1000 to 10 hPa with 17 pressure levels and includes sea-level pressure, air temperature, geopotential height and wind fields. In addition, we also checked the Global Historical Climatology Network (GHCN) data set and the CRUTem data set, which is derived from air temperatures near to the land surface. Because the GHCN station count

has recently decreased, the representativeness of the data is also reduced, and the CRUTem cannot be used to obtain WCT information because it does not include wind velocity data. However, the spatial distribution of winter temperature trends over Northern Asia via the CRUTem verifies the spatial distribution of winter WCT trends in our study.

To ensure all data were of reasonable quality and to protect the quality of further analysis, data quality control was performed. The data quality control process is described as follows. (1) After screening all daily temperature and wind speed records for 24 594 stations, only the data in the period from 1973 to 2013 were analysed in this study because the records are relatively complete. (2) For a given station and a given month, any station missing data from more than ten records of air temperature or wind velocity was excluded. (3) According to the application scope of WCT, stations with monthly air temperatures above 10 °C were removed. After data quality control, 381 stations were finally selected for analysis.

The wind chill formula used in this study was proposed in 2002 in a cooperative work by the Meteorological Services of Canada, the US National Weather Service, and several other members of academic research collectives (National Weather Service, 2001). This formula is applied when air temperature is no more than 10 °C (Bluestein and Osczevski, 2002; Osczevski and Bluestein, 2005). Recently, Canada improved the wind chill formulas (Government of Canada, 2015). One of the largest differences in the wind chill formulas used in 2002 and 2015 is the limit of application. In contrast with the 2002 formula (Osczevski and Bluestein, 2005), the 2015 formula is used when air temperature is no more than 0 °C because Northern Asia (including China and Mongolia) is located in the mid-latitudes and the 0 °C is low to calculate WCT. Thus, the 2002 formula is more suitable for this study, and WCT was computed according to the formula shown in Equation (1) (Osczevski and Bluestein, 2005) as follows:

$$\text{WCT} = 13.12 + 0.6215 \times T\text{-}11.37 \times V_{10\,\text{m}}^{0.16}$$
$$+ 0.3965 \times T \times V_{10\,\text{m}}^{0.16} \quad (1)$$

where T is air temperature in °C, and V is wind speed at 10 m above the ground measured by a weathervane in km h^{-1}. This formula can be applied for a temperature range from −50 to 10 °C and wind speeds greater than 4.8 km h^{-1}. Under the condition of missing records for air temperature or wind velocity, WCT was calculated as follows. (1) WCT is considered a missing value if either the air temperature or wind speed is missing. (2) The value of air temperature is treated as WCT if the wind speed record is less than 4.8 km h^{-1} on that day (Shitzer and de Dear, 2006).

Finally, to examine whether a WCT warming hiatus occurred over Northern Asia, following Duan and Xiao (2015) and Li *et al.* (2015), we divided the analysed period into two sub-periods, i.e. 1973–1998 (P1) and 1999–2013 (P2), and a least squares method was used to obtain the long-term WCT trend. In addition, to explain the reasons

for the changes in WCT trends, the long-term trends in air temperature and wind speed were also calculated and the partial regression coefficient of air temperature (wind speed) solely to winter WCT variations were estimated.

The partial regression coefficient of air temperature (wind speed) to winter WCT variations is obtained as follows: (1) WCT was regressed with respect to wind speed (air temperature) and the residuals were used to represent the wind speed-free (air temperature-free) components. (2) The square of the correlation coefficient between the wind speed-free (air temperature-free) components and air temperature (wind speed) is treated as the partial regression coefficient of air temperature (wind speed) to WCT changes. It should be noted that the interactions between air temperature and wind speed (which might influence the partial regression coefficient of air temperature and wind speed relative to the WCT changes) are not considered, and this method is only a rough estimate. All variables analysed in this study are applicable to the winter season (December, January and February).

3. Results

3.1. Winter WCT trend over Northern Asia

Figure 1 shows the spatial distribution of the winter WCT trends over Northern Asia for the entire analysed period and for the two sub-periods. For the entire analysed period (Figure 1(a)), the winter WCT displays a warming trend over the majority of Northern Asia. Of all 381 stations, more than 300 stations present a warming trend. Most of the stations exhibit relatively significant upward trends exceeding $1\,°C\,decade^{-1}$ over South Korea, northeastern China, Northern China and the Tibetan Plateau (TP), and those over Western Siberia and Japan show relatively weak values with an interval of 0 to $0.5\,°C\,decade^{-1}$. We also examined the WCT trends during the two sub-periods, i.e. 1973–1998 (P1) and 1999–2013 (P2). In the P1 epoch, WCT still shows upward trends over Northern Asia, particularly in central China and northeastern China. Nearly half of the stations display WCT trends exceeding $1\,°C\,decade^{-1}$ (Figure 1(b)) compared with 381 stations during over the entire analysed period. Comparing Figure 1(a) and (b), the increasing trends are higher over most regions during the P1 period than during the entire analysed period, especially in Japan, Korea, northeastern China, central China and Mongolia. Nearly 89% of stations exhibit higher tendencies for winter WCT during the P1 epoch than during the entire analysed period. We averaged WCT over Northern Asia for the entire period and the P1 period and calculated their WCT trends. The WCT trend over Northern Asia is $+0.35 \pm 0.29\,°C\,decade^{-1}$ for the period of 1973–2013, but it increases during P1 with a value of $+1.18 \pm 0.47\,°C\,decade^{-1}$. The WCT trends for both the entire analysed period and the P1 period are significant at the 95% confidence level. Similarly, the spatial distribution of the WCT trends in P2 is shown. The WCT trends in most regions show a reverse spatial pattern during the P2 period compared with the P1 period

because many significant downward trends occur over Northern Asia, except for the Far East (FE) in Russia, Northern Japan and the TP. Among the stations, nearly 33% show a decreasing trend of less than $-1\,°C\,decade^{-1}$. For other regions, amplified warming tendencies in WCT are noted over the FE in Russia and Northern Japan and weak warming trends are observed over the TP in P2 compared with P1. To examine the spatial distribution of the WCT trends in the P2 period, we divided the stations into three categories, i.e. the FE, the TP and other regions in Northern Asia (RA). It should be noted that the FE cannot stand for all high latitudes and the TP only represents the eastern Tibetan Plateau because the stations are distributed sparsely. Additionally, we calculated the trends for P1 and P2. During the P1 (P2) period, the winter WCT trends are $0.54 \pm 0.64\,°C\,decade^{-1}$ ($0.75 \pm 1.41\,°C\,decade^{-1}$), $0.67 \pm 0.42\,°C\,decade^{-1}$ ($-0.04 \pm 1.10\,°C\,decade^{-1}$) and $1.11 \pm 0.52\,°C\,decade^{-1}$ ($-1.02 \pm 1.7\,°C\,decade^{-1}$) for the FE, the TP and RA, respectively (Figure 2). Based on the changes in the WCT trend from P1 to P2 over these three regions, the warming hiatus of WCT occurs over the TP and RA other than the FE during P2. Previous studies (Li *et al.*, 2015) reported that the surface air temperature over RA experienced a warming slowdown during P2 compared with P1, and the trends in surface air temperature are 0.80 and $-0.85\,°C\,decade^{-1}$ for P1 and P2, respectively. However, no warming hiatus of surface air temperature occurs over the TP because its trends are 0.21 and $0.47\,°C\,decade^{-1}$ during P1 and P2, respectively (Duan and Xiao, 2015; Li *et al.*, 2015). Comparing the changes in the trend of WCT and surface air temperature for the TP and RA, the warming hiatus of surface air temperature over RA might explain the slowdown of WCT in those locations. However, for the TP, the warming hiatus of WCT is in line with a significant increase in the upward trend in surface air temperature from P1 to P2, which might be caused by the changes in wind speed. The details are clarified in the next section.

3.2. Contributions of surface air temperature and wind speed to changes in winter WCT

Following the formula of WCT, the impact of changes in air temperature and wind velocity on the WCT variations was evaluated. In this work, trends in winter air temperature and wind velocity are discussed to clarify the changes in the WCT trend in Northern Asia. As shown in Figure 3, a significant upward trend in air temperature occurs over the TP, the FE and RA during P1, with values of 0.24 ± 0.40, 0.52 ± 0.54, and $0.8 \pm 0.46\,°C\,decade^{-1}$, respectively. Wind velocities show decreasing trends during P1 for the TP, the FE and RA with trends of -0.28 ± 0.06, -0.04 ± 0.09, and $-0.17 \pm 0.06\,m \cdot s^{-1}\,decade^{-1}$, respectively. The increasing air temperature and decreasing wind speed drive an increasing WCT during P1 over the mid to high latitudes of Asia. However, during P2, air temperature shows different trends for these regions, with an upward trend of 0.49 ± 0.98 and $0.52 \pm 1.14\,°C\,decade^{-1}$ over the TP and FE, respectively, and a downward trend
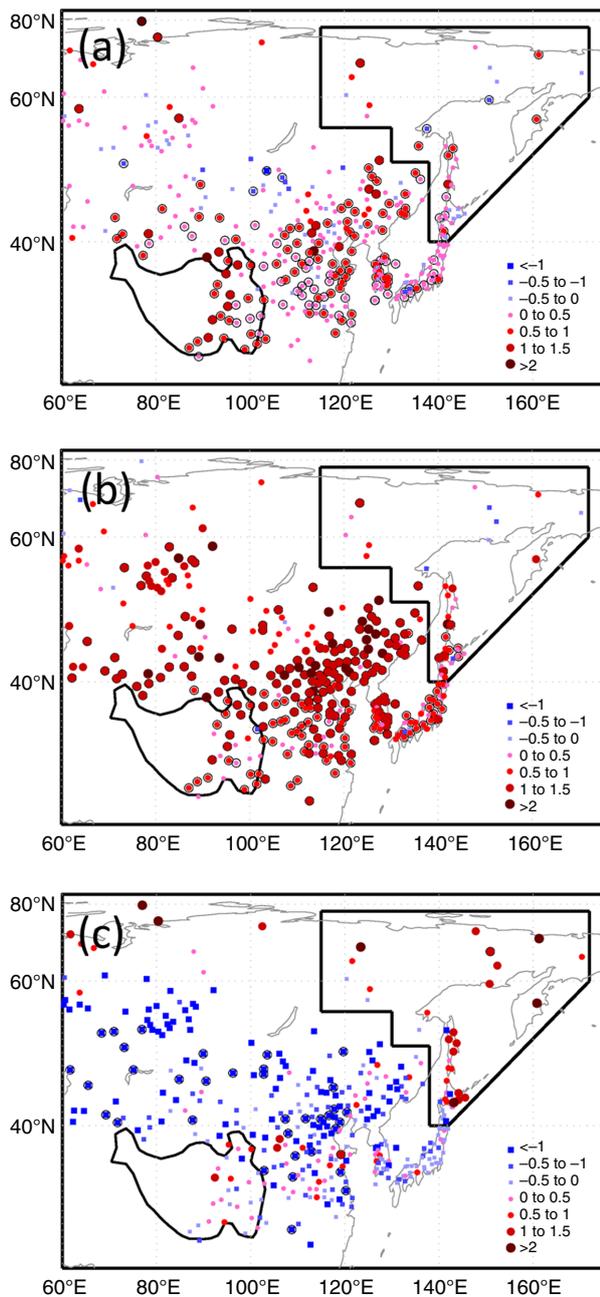
Figure 1. Spatial distribution of winter WCT trends over Northern Asia: (a) Period 1973–2013, (b) period 1973–1998 and (c) period 1999–2013. The circled points indicate that trends are significant at the 95% confidence level. Units: °C decade^{-1}. Stations enclosed by solid contour line on the left of the map belong to the TP and on the right of the map belong to the FE. [Colour figure can be viewed at wileyonlinelibrary.com].
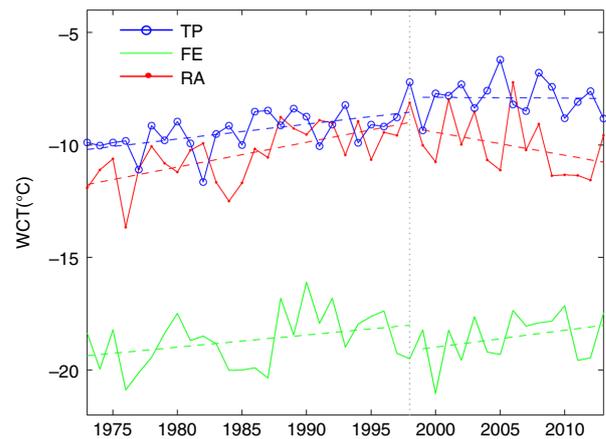

Figure 2. Anomaly time series of average winter WCT over the TP (open circle), FE and RA (solid circle). Dashed lines indicate the linear trends. [Colour figure can be viewed at wileyonlinelibrary.com].

epoch. For the FE, the WCT trend is determined by an increasing trend in air temperature and a nearly zero trend in wind velocity, resulting in an increasing WCT trend in the P2 period. Comparison of the changes in WCT trends from P1 to P2 for these three regions reveals that a warming hiatus of WCT occurs over the TP and RA during recent decades.

To determine the effect of air temperature and wind speed on WCT changes, the partial regression coefficient of air temperature and wind velocity to the WCT trend were further examined. We derived the wind-free (air temperature-free) component of the WCT time series by regression analysis and calculated the square of the correlation coefficient between the wind speed-free (air temperature-free) component and air temperature (wind speed), which is treated as the partial regression coefficient of air temperature (wind speed) to WCT changes (for details, see Section 2). The results show that the partial regression coefficients (Table 1) of wind speed (air temperature) to winter WCT are 14.44% (89.67%), 1.03% (97.48%) and 1.43% (56.26%) during P1 for the TP, the FE and RA, respectively. During P2, the partial regression coefficients of wind speed (air temperature) to the winter WCT are 10.84% (84.11%), 0.69% (84.94%) and 0.77% (96%), respectively, for the TP, the FE and RA. According to the partial regression coefficients, we conclude that the surface air temperature plays a dominant role in the winter WCT variation over the mid to high latitudes in Northern Asia from P1 to P2. Among the regions, changes in wind speed over the TP contribute more significantly to WCT variations compared with other regions. For example, the upward trend in wind speed during the P2 period offsets the increasing trend in surface air temperature, and as a result, WCT shows a nearly zero trend over the TP.

4. Reasons for winter WCT variations over Northern Asia

In this section, we analyse the atmospheric circulation changes and discuss the reasons for the changes in the

of $-0.85 \pm 1.51\,°C\,decade^{-1}$ over RA. At the same time, an increasing trend in wind velocity is observed for the TP by a value of $0.33 \pm 0.16\,m\cdot s^{-1}\,decade^{-1}$ (significant at the 95% confidence level) in the P2 period, and nearly zero trends are noted for wind velocity over RA and the FE. Because the increasing wind velocity offsets the increasing air temperature over the TP, the TP experiences a nearly unchanged WCT during the P2 period. RA shows a downward trend in WCT due to decreasing trends in air temperature and unchanged wind velocity during the P2
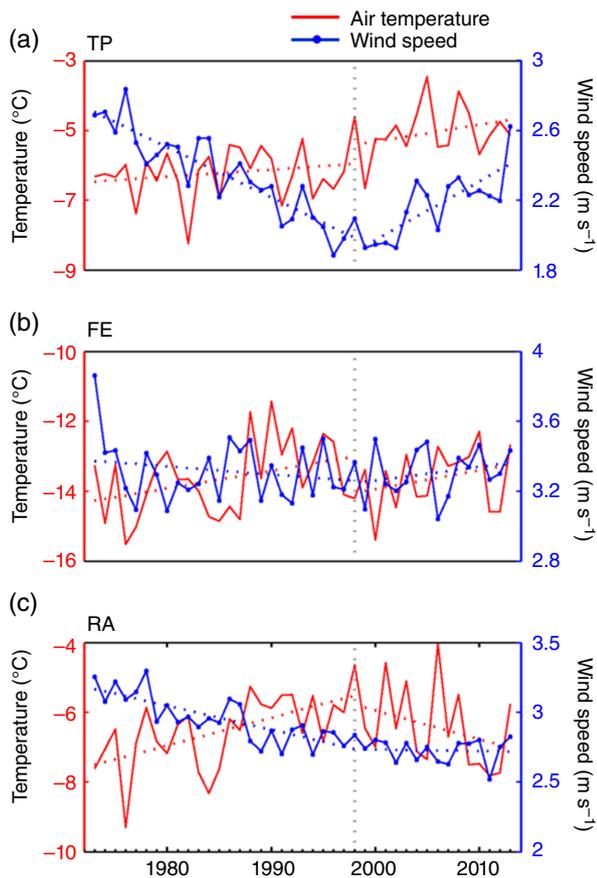
Figure 3. Time series of average air temperature and wind speed (solid circle) in winter (DJF) over TP (a), FE (b) and RA (c). Dashed lines indicate the linear trends. [Colour figure can be viewed at wileyonlinelibrary.com].

trend of the winter WCT over Northern Asia. As background for changes in surface air temperature and wind speed, atmospheric circulation anomalies result in winter WCT variations over Northern Asia. To reveal the changes in atmospheric circulation, composites of the wind field at 925 hPa, the geopotential height at 500 hPa, and the sea-level pressure during winter season were analysed between P1 and P2.

As shown in the Figure 4(a), a large area of positive anomaly covers the middle to high latitudes in Asia, with an anomalous centre located to the north of Western Siberia ($60°–80°$N and $60°–100°$E) during P2. The pressure gradient between the Siberian high and central China indicates an increased northerly wind anomaly across East Asia, which is also favourable for cold air transporting from the high latitudes to middle latitude. Figure 4(b) shows the geopotential height anomaly at 500-hPa level and the wind field anomaly at 925-hPa level during P2. Positive anomalies occur, covering the high-latitude region in Asia, and a negative height anomaly is observed over Baikal in the mid-troposphere. The gradient of enhanced pressure in the high-latitude region and the reduced pressure in the mid-latitude regions result in an increased driving force for air mass transfer, which is supported by the northerly wind anomalies over the high to mid latitudes in Asia, as revealed by the wind field composite at the 925-hPa level. Therefore, the cold air over the Arctic transported to the middle latitudes caused reduced temperature over RA during P2. The warming causes for P1 are opposite to the patterns described above.

For the TP, due to high elevation, the increasing air temperature might be determined more significantly by solar radiation and cloud changes (Zhang and Zhou, 2009; Guo and Wang, 2012), but it should be noted that solar radiation has declined since 1980 over the TP (Tang *et al.*, 2011), which might be attributed to increasing water vapour and deep (but not total) cloud cover (Yang *et al.*, 2012). Thus, solar radiation cannot explain the continuous warming over the TP. Duan and Xiao (2015) postulated that cloud-radiation feedback might partially explain the temperature increase over the southern TP. Decreased clouds in the daytime could increase the sunshine duration, whereas strengthened clouds at night could heat air through the cloud heat preservation effect. However, Duan and Xiao (2015) did not give a possible reason for the increasing air temperature in the northern TP. Thus, an explanation for the increasing air temperature over the TP might require further analysis. In addition, Lin *et al.*

Table 1. Trends in air temperature, wind velocity and WCT. The sixth and seventh columns indicate the partial regression coefficient of air temperature and wind velocity on the trend of WCT, respectively.

Period	Region	T	V	WCT	T contribution	V contribution
1973–1998	TP	0.21	−0.29 **	0.67 **	0.8967	0.1444
	FE	0.51 *	−0.05	0.54 *	0.9748	0.0103
	RA	0.80 **	−0.17 **	1.11 **	0.5626	0.0143
1999–2013	TP	0.47	0.34 **	−0.04	0.8411	0.1084
	FE	0.54	0.08	0.75	0.8494	0.0069
	RA	−0.83	−0.01	−1.02	0.96	0.0077
1973–2013	TP	0.48 **	−0.12 **	0.67 **	0.8038	0.0833
	FE	0.16	−0.01	0.23	0.9757	0.0101
	RA	0.19	−0.12 **	0.34 *	0.8178	0.0225

The unit of T trend and WCT trend is °C decade^{-1}, and the unit of V trend is m·s^{-1} decade^{-1}. (T is short for temperature and V is short for wind speed.) T contribution and V contribution are the contribution ratios of temperature and wind. TP means Tibetan Plateau, FE means the Far East and RA means the rest of Northern Asia. *Indicates the trend is significant at 90% confidence level. **Indicates the trend is significant at 99% confidence level.
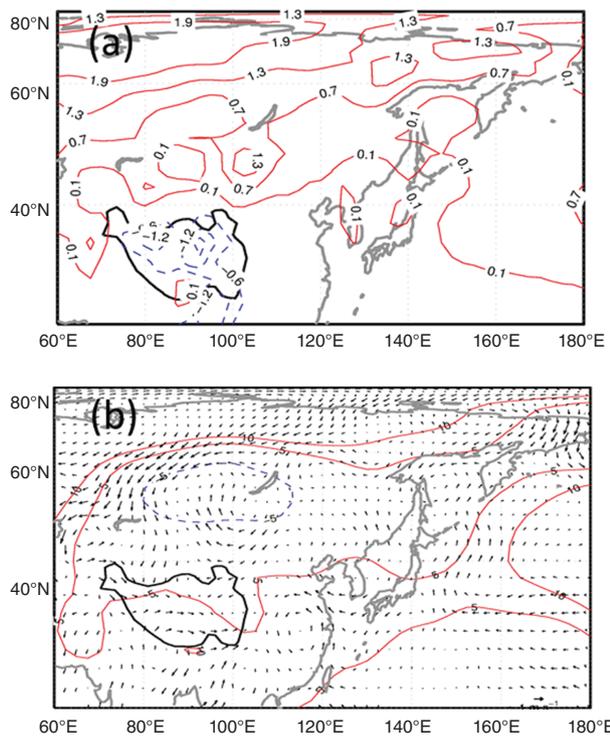
Figure 4. Sea-level pressure (a) (1999–2013 minus 1973–2013). And composite of winter (DJF) (b) 500-hPa geopotential height and 925-hPa wind field (m·s⁻¹) (1999–2013 minus 1973–2013). Contour intervals are 1 hPa in (a), 1 hPa in (b). Dashed are negative, solid lines indicates positive. The shaded is statistically significant at the 95% confidence level. The bold curve indicates the TP. [Colour figure can be viewed at wileyonlinelibrary.com].
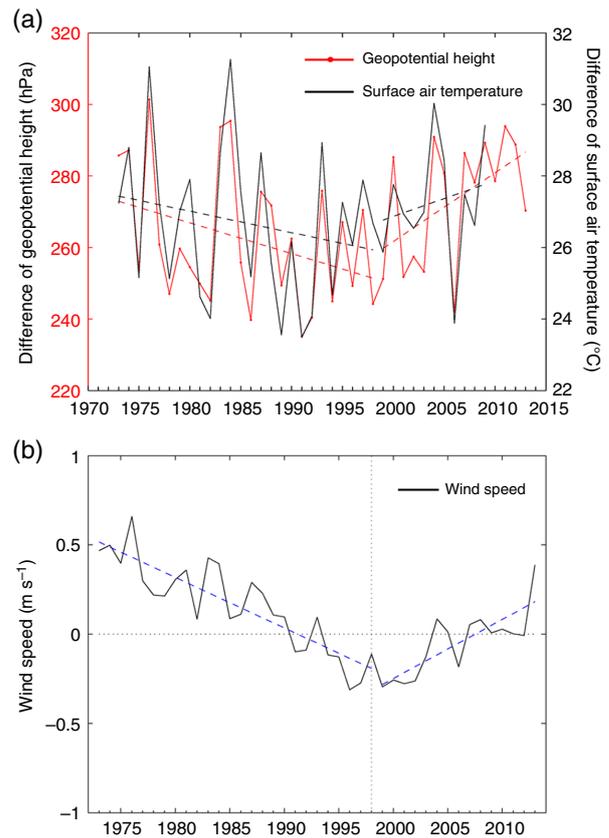

Figure 5. Difference of winter geopotential height (solid circle) at 500-hPa level (1973–2013) and surface air temperature (1973–2009) (a) between region 1 (20°–25°N, 80°–102.5°E) and region 2 (45°–50°N, 80°–102.5°E). Dashed lines indicate the trend for pre-1998 and post-1999 (b). [Colour figure can be viewed at wileyonlinelibrary.com].

(2013) reported that wind speed was changed by the gradient of the 500-hPa geopotential height through transport momentum, and the gradient of the 500-hPa geopotential height was altered by the surface warming rate through atmospheric thermal adaption. To test whether the theory fits the observations in the TP during 1973–2013, we calculated the gradients of the 500-hPa geopotential height and temperature in regions of the north (40°–50°N, 80°–102.5°E) and south (20°–25°N, 80°–102.5°E) of the TP. As shown in Figure 5(a), the trends of the gradient of surface air temperature and the gradient of the 500-hPa geopotential height are similar, with a correlation coefficient of 0.85. The notably large surface temperature reflects the latitudinal difference in surface warming, which results in the gradient of the 500-hPa geopotential height through thermal adaption. Owing to the change in atmospheric circulation, the wind variation in the TP closely corresponds to the trend in the gradient of the 500-hPa geopotential height, i.e. the 500-hPa geopotential height decreases before 1998 and increases after 1999, which has an effect on the variation of wind speed. Therefore, wind speed in the TP might be a consequence of the gradient in surface air temperature. For the FE, through the wind field at the 925-hPa level (Figure 4(d)), a warm air mass with easterly wind and southerly wind from the Western Pacific at the surface affects the warm air temperature over the FE during P2.

5. Conclusions

Based on observational data from 1973–2013, we investigated the changes in the trends of the winter WCT over the TP, the FE and the rest of Northern Asia (RA). The results show that compared with the increasing trend in WCT during 1973–1998 (P1) over Northern Asia, winter WCT experienced a warming hiatus in the TP and RA from 1999 to 2013 (P2), and the cooling tendency over RA during P2 is significant. For the FE, winter WCT continued to heat up. The causes of the winter WCT variation over the TP, the FE and RA are different. Over RA, the temperature plays a dominant role in the winter WCT trend (Table 1). Further analysis indicates that the hiatus of winter WCT over RA is a result of atmospheric circulation anomalies in the low- and mid-troposphere. Compared with the circulation in the P1 epoch, positive height anomalies occur over Siberia and negative height anomalies occur over the area in the north of the TP (western Mongolia) during P2 at sea-level pressure (500 hPa). This distribution of height anomalies results in an increased pressure gradient from high latitude to middle latitude during P2, which is favourable for cold air to transport from high latitude to middle latitude, and creates a low air temperature over these regions. Over the TP, both temperature and wind speed are important to the

winter WCT trend. The temperature continues to rise during the P1 and P2 periods; however, wind speed presents a decreasing (increasing) trend during the P1 (P2) period. The increase in wind velocity offsets the increase in air temperature during the P2 period, resulting in a nearly zero trend in WCT and a slowdown compared with the increasing WCT the P1 period. The increase in temperature over the southern TP might be caused by a decrease (increase) in the daytime (night-time) cloud amount (Duan and Xiao, 2015), but an explanation for the increasing air temperature over the whole TP requires further analysis. The increase in wind velocity during P2 might be caused by the increasing height gradient and air temperature between the regions to the south and to the north of the TP at the 500-hPa level, which results in increased wind velocity due to atmospheric thermal adaption. For the FE, southerly wind and easterly wind anomalies from Western Pacific cause the temperature to increase during the P2 period through warm advection.

References

Analitis A, Katsouyanni K, Biggeri A, Baccini M, Forsberg B, Bisanti L, Kirchmayer U, Ballester F, Cadum E, Goodman PG, Hojs A, Sunyer J, Tiittanen P, Michelozzi P. 2008. Effects of cold weather on mortality: results from 15 European cities within the PHEWE project. *Am. J. Epidemiol.* **168**(12): 1397–1408.

Baccini M, Biggeri A, Accetta G, Kosatsky T, Katsouyanni K, Analitis A, Anderson HR, Bisanti L, D'Ippoliti D, Danova J, Forsberg B, Medina S, Paldy A, Rabczenko D, Schindler C, Michelozzi P. 2008. Heat effects on mortality in 15 European cities. *Epidemiology* **19**(5): 711–719, doi: 10.1097/Ede.0b013e318176bfcd.

Balafoutis CJ. 1989. Diurnal-variation of wind-chill at Thessaloniki, Greece. *Int. J. Biometeorol.* **33**(4): 266–271, doi: 10.1007/Bf01051088.

Bluestein M, Osczevski R. The basis for the new wind chill temperature chart. 2002. In *Preprints, 15th Conference on Biometeorology/Aerobiology and 16th International Congress of Biometeorology*, Kansas City, KS, American Meteorological Society CD-ROM, 6B.1.

Czarnecka M, Michalska B. 2007. Perception of weather conditions during atmospheric thaw in the Szczecin Lowlands. *Int. Agrophys.* **21**(1): 29–37.

Danielsson U. 1996. Windchill and the risk of tissue freezing. *J. Appl. Physiol.* **81**(6): 2666–2673.

Duan AM, Xiao ZX. 2015. Does the climate warming hiatus exist over the Tibetan Plateau? *Sci. Rep.* **5**: 13711. 10.1038/srep13711.

Easterling DR, Wehner MF. 2009. Is the climate warming or cooling? *Geophys. Res. Lett.* **36**: L08706, doi: 10.1029/2009GL037810.

Feng SH, Gong DY, Zhang ZY, He XZ, Guo D, Lei YN. 2009. Wind-chill temperature changes in winter over China during the last 50 years. *Acta Geogr. Sin.* **64**: 12.

Fyfe JC, Gillett NP, Zwiers FW. 2013. Overestimated global warming over the past 20 years. *Nat. Clim. Change* **3**(9): 767–769.

Fyfe JC, Meehl GA, England MH, Mann ME, Santer BD, Flato GM, Hawkins E, Gillett NP, Xie S-P, Kosaka Y, Swart NC. 2016. Making sense of the early-2000s warming slowdown. *Nat. Clim. Change* **6**(3): 224–228, doi: 10.1038/nclimate2938.

Government of Canada. 2015. *Climate glossary: wind chill.* http://climate.weather.gc.ca/glossary_e.html (accessed 22 June 2016).

Guo DL, Wang HJ. 2012. The significant climate warming in the northern Tibetan Plateau and its possible causes. *Int. J. Climatol.* **32**: 1775–1781.

IPCC. 2013. Summary for policymakers. In *Climate Change 2013: The Physical Science Basis. Contribution of Working Group I to the Fifth Assessment Report of the Intergovernmental Panel on Climate Change* Stocker TF, Qin D, Plattner G-K, Tignor M, Allen SK, Boschung J, Nauels A, Xia Y, Bex V, Midgley PM (eds). Cambridge University Press: Cambridge, UK and New York, NY, 3–30.

Kalnay E, Kanamitsu M, Kistler R, Collins W, Deaven D, Gandin L, Iredell M, Saha S, Whithe G, Woollen J, Zhu Y, Chellian M, Ebisuzaki W, Higgins W, Janowiak J, Mo KC, Ropelewski C, Wang J, Leetmaa A, Reynolds R, Jenne R, Joseph D. 1996. The NCEP/NCAR 40-year reanalysis project. *Bull. Am. Meteorol. Soc.* **77**: 437–471.

Keimig FT, Bradley RS. 2002. Recent changes in wind chill temperatures at high latitudes in North America. *Geophys. Res. Lett.* **29**(8): 4-1–4-4, doi: 10.1029/2001GL013228.

Kosaka Y, Xie SP. 2013. Recent global-warming hiatus tied to equatorial Pacific surface cooling. *Nature* **501**: 403–407, doi: 10.1038/nature12534.

Li Q, Yang S, Xu W, Wang XL, Jones P, Parker D, Zhou L, Feng Y, Gao Y. 2015. China experiencing the recent warming hiatus. *Geophys. Res. Lett.* **42**(3): 889–898, doi: 10.1002/2014gl062773.

Lin CG, Yang K, Qin J, Fu R. 2013. Observed coherent trends of surface and upper-air wind speed over China since 1960. *J. Clim.* **26**(9): 2891–2903, doi: 10.1175/Jcli-D-12-00093.1.

National Weather Service, 2001. *NWS windchill chart.* http://www.nws.noaa.gov/om/winter/faqs.shtml (accessed 1 January 2011).

Osczevski R, Bluestein M. 2005. The new wind chill equivalent temperature chart. *J. Bull. Am. Meteorol. Soc.* **86**: 1453–1458.

Rehill N, Armstrong B, Wilkinson P. 2015. Clarifying life lost due to cold and heat: a new approach using annual time series. *BMJ Open* **5**(4): e005640.

Shitzer A, de Dear R. 2006. Inconsistencies in the 'new' windchill chart at low wind speeds. *J. Appl. Meteorol. Climatol.* **45**: 787–790.

Siple PA, Passel CF. 1945. Measurements of dry atmospheric cooling in subfreezing temperatures. *Am. Philos. Soc.* **89**(1): 23.

Tang W, Yang K, Qin J, Cheng C, He J. 2011. Solar radiation trend across China in recent decades: a revisit with quality-controlled data. *Atmos. Chem. Phys.* **11**: 393–406, doi: 10.5194/acp-11-393-2011.

Tiffany A. 2016. Deaths, travel disruption as bitter cold grips Asia. http://edition.cnn.com/2016/01/25/asia/asia-cold-weather-travel-disruption/ (accessed 25 January 2016).

Trenberth KE, Fasullo JT, Branstator G, Phillips AS. 2014. Seasonal aspects of the recent pause in surface warming. *Nat. Clim. Change* **4**(10): 911–916, doi: 10.1038/Nclimate2341.

Vautard R, Cattiaux J, Yiou P, Thepaut JN, Ciais P. 2010. Northern Hemisphere atmospheric stilling partly attributed to an increase in surface roughness. *Nat. Geosci.* **3**(11): 756–761, doi: 10.1038/NGEO979.

Yang K, Ding B, Qin J, Tang W, Lu N, Lin C. 2012. Can aerosol loading explain the solar dimming over the Tibetan Plateau? *Geophys. Res. Lett.* **39**(20): L20710, doi: 10.1029/2012GL053733.

Zhang RH, Zhou SW. 2009. Air Temperature changes over the Tibetan Plateau and other regions in the same latitudes and the role of ozone depletion. *Acta Meteorol. Sin.* **23**: 290–299.